Clinical Biomechanics 105 (2023) 105983

Contents lists available at ScienceDirect

Clinical Biomechanics

journal homepage: www.elsevier.com/locate/clinbiomech

Gait analysis of leprosy patients with foot drop using principal component analysis

Jose Carlos Cohen [a], Adriane Mara de Souza Muniz [b,c], Roberto B. Carvalho Junior [b], Henrique Lelis Clemente de Oliveira [b], Silvana T. Miranda [a], Maria Kátia Gomes [a], Antonio José Ledo Alves da Cunha [d], Luciano L. Menegaldo [b,*]

[a] Hospital Universitário, Universidade Federal do Rio de Janeiro (UFRJ), Brazil
[b] Programa de Engenharia Biomédica (PEB/COPPE), Universidade Federal do Rio de Janeiro (UFRJ), Brazil
[c] Escola de Educação Física do Exército (EsEFEx) – (Brazilian Army), Brazil
[d] Programa de Pós-Graduação em Clínica Médica, Faculdade de Medicina, Universidade Federal do Rio de Janeiro, Brazil

A R T I C L E I N F O

Keywords:
Principal component analysis
Leprosy
Foot drop
Gait analysis
Hansen's disease

A B S T R A C T

Background: Peripheral nerve injury caused by leprosy can lead to foot drop, resulting in an altered gait pattern that has not been previously described using 3D gait analysis.
Methods: Gait kinematics and dynamics were analyzed in 12 patients with unilateral foot drop caused by leprosy and in 15 healthy controls. Biomechanical data from patients' affected and unaffected limbs were compared with controls using inferential statistics and a standard distance, based on principal components analysis (PCA).
Findings: Patients walked slower than controls (0.8 ± 0.2 vs. 1.1 ± 0.2 m/s, $p = 0.003$), with a reduced stance and increased swing percentage. The affected limb increased ($p < 0.05$) plantar flexion at the initial contact (−16.8° ± 8.3), terminal stance (−29.1° ± 11.5), and swing (−12.4° ± 6.2) in the affected limb compared to unaffected (−6.6° ± 10.3; −14.6° ± 11.6; 2.4° ± 7.6) and controls (−5.4° ± 2.5; −18.8° ± 5.8; −1.4° ± 3.9). Increased pelvic tilt and knee adduction/abduction range, with lower hip adduction, were observed. The second peak of ground reaction force (98.6 ± 5.2 %BW), ankle torque (0.99 ± 0.33 Nm/kg), and net ankle work in stance (−0.03 ± 5.4 J/Kg) decreased in the affected limb compared to controls (104.1 ± 5.5 %BW; 1.24 ± 0.4 Nm/kg; −4.58 ± 5.19 J/kg; $p < 0.05$). There were decreasing multivariate standard distances in the affected limb compared with the unaffected and controls. PCA loading factors highlighted the major differences between groups.
Interpretation: Leprosy patients with foot drop presented altered gait patterns in affected and unaffected limbs. There were remarkable differences in ankle kinematics and dynamics. Rehabilitation devices, such as ankle foot orthosis or tendon transfer surgeries to increase ankle dorsiflexion, could benefit these patients and reduce deviations from normal gait.

1. Introduction

Leprosy, or Hansen's disease, is a chronic infectious and neglected disease caused by *mycobacterium leprae* (Hambridge et al., 2021). In 2019, there were 202,185 new cases reported worldwide, with Brazil ranked second with 27,863 new cases, the highest in the Americas (WHO, 2020). Nerve injury is a significant feature of leprosy pathogenesis, as *Mycobacterium leprae* has a unique tendency to invade Schwann cells in the peripheral nervous system. As a result, immunologic mononeuritis multiplex occurs, causing autonomic, sensory, and motor neuropathy (Wilder-Smith and Van Brakel, 2008). Despite receiving antileprosy treatment and recovering from the infection, many patients still suffer permanent nerve damage and disabilities (Sharma et al., 1996). This impairment is irreversible, and motor nerve conduction studies using electroneuromyography show a complete absence of electric activity (Marciniak, 2013).

The compromise of the common peroneal nerve often leads to foot drop due to leprosy (Ooi and Srinivasan, 2004; Wilder-Smith and Van Brakel, 2008). Symptoms include a characteristic steppage gait, permanent loss of the leg's anterior and lateral compartments, and impaired

* Corresponding author at: Av Horácio Macedo, 2030 – CT- Bloco H – 338, 21941-914, Rio de Janeiro, RJ, Brazil.
E-mail address: lmeneg@peb.ufrj.br (L.L. Menegaldo).

https://doi.org/10.1016/j.clinbiomech.2023.105983
Received 26 December 2022; Accepted 1 May 2023
Available online 4 May 2023
0268-0033/

muscle function (Krishnamurthy and Ibrahim, 2019). This damage results in a significant alteration of the walking pattern, general impairment of the swing, and muscle weakness, with shortening and contracture of the Achilles tendon as a secondary effect (Beckmann et al., 2015).

Foot drop is a condition that refers to weakness in dorsiflexion and can occur in various conditions, including injury of the peroneal nerve, L5 radiculopathy (Marciniak, 2013; Poage et al., 2016), muscular pathologies, such as Duchenne muscular dystrophy (Goudriaan et al., 2018), hereditary peripheral neuropathy such as Charcot-Marie-Tooth (Don et al., 2007; Ferrarin et al., 2013), post-stroke (Balaban and Tok, 2014; Pinzur et al., 1987), and cerebral palsy (Karunakaran et al., 2019). Newman et al. (2007) observed foot drop during the swing phase, reduced plantar flexion at push-off, and increased foot supination in patients with Charcot-Marie-Tooth gait pattern. Voigt and Sinkjaer (2000) described foot drop walking dynamics in hemiplegic patients, focusing primarily on estimated bone-to-bone contact forces in the ankle, knee and hip with and without a peroneal nerve stimulator.

Reduced gait speed, cadence, and stride length, with increased stride and step times, are common findings in patients with foot drop. These findings are associated with limited ankle dorsiflexion and hyperextension of the knee at initial contact (Balaban and Tok, 2014; Błażkiewicz et al., 2017). Additionally, reduced hip extension at propulsion and increased hip flexion during swing on the affected leg have also been reported (Błażkiewicz et al., 2017). Patients with foot drop also experience reduced dorsiflexor torque, hip extension and flexion torques, and flexor knee torque. In contrast, Simonsen et al. (2010) observed a significant increase in the knee extensor moment in the affected leg of subjects with foot drop. Błażkiewicz and Wit (2019) reported increased knee and hip flexors, extensors, and adductors forces to compensate for the loss of ankle muscle forces in patients with foot drop.

Although several diseases can cause foot drop, the specific etiology associated with leprosy can result in specific abnormal gait patterns. However, to the best of the authors' knowledge, no previous study has characterized the gait patterns associated with foot drop caused by leprosy using 3D gait analysis techniques, despite its relatively high occurrence in developing countries. Quantitatively evaluating musculoskeletal damage can aid in the planning and monitoring of rehabilitation and surgery. This gap in the literature is partly due to the scarcity of public-supported gait analysis laboratories in developing countries, which is associated with the low social and economic status of individuals affected by leprosy. This makes it challenging to afford sophisticated diagnostic technology and participate in clinical studies.

This study aims to describe the gait characteristics of leprosy patients with common peroneal nerve damage and foot drop using 3D motion analysis. Inferential and multivariate statistical methods, including principal component analysis (PCA), were used to characterize gait parameters between the affected and non-affected legs of patients with leprosy and between the affected leg and healthy controls. The results of this study improve our understanding of the gait characteristics of foot drop resulting from leprosy and serve as a baseline for comparison after physical therapy and surgical interventions, such as tendon transfers. We hypothesized that leprosy patients might exhibit reduced dorsiflexion motion during swing and decreased plantar flexor moment during late stance.

2. Materials and methods

2.1. Sample

The sample size for comparing leprosy and foot drop as a secondary disability (Hansen Group - HG) with a Control Group (CG) was calculated using an independent samples *t*-test model. An effect size of $d > 1.30$ (large effect), with a significance level of $\alpha < 0.05$ and a power of 0.80, was chosen. The G*Power statistical package (Faul et al., 2007) was utilized for this purpose. The effect size was determined based on the largest variability in sagittal plane kinematics, specifically the ankle at initial contact, as reported by Błażkiewicz et al. (2017). This calculation yielded a minimum sample size of nine participants.

The HG consisted of twelve patients selected from the Orthopedic Clinic of Clementino Fraga Filho University Hospital, including eight men with an average age of 44.7 ± 10.8 years, a height of 1.7 ± 0.08 m, and a body mass of 82.6 ± 20 kg. All subjects completed multidrug therapy according to the Brazilian Health Ministry protocol (Ministério da Saúde, 2020) and had not experienced any inflammatory reaction within the previous year. The inclusion criteria for this study were the presence of foot drop, minimum age of 18 years, and the absence of any limb deformity or previous surgeries except for tibial or common peroneal nerve neurolysis. Active plantar ulcers or foot infections constituted exclusion criteria. Additionally, a control group (CG) comprised 15 healthy volunteers (12 men; 37.6 ± 15.6 years; 1.7 ± 0.06 m; 74.5 ± 18.6 kg). The groups had no significant differences in age and anthropometrics ($p > 0.05$). All volunteers provided informed consent, and the Local Ethics Committee approved the study (CAAE no. 24952119.0.0000.5257).

2.2. Experimental protocol

A system consisting of four BTS P-6000 force platforms (BTS Bioengineering, Milan, Italy) with a sampling frequency of 400 Hz and seven infrared cameras (SMART-D BTS, Milan, Italy) with a sampling frequency of 250 Hz was used for 3D gait analysis. The marker set used was the Helen Hayes protocol with 18 reflective markers (Kadaba et al., 1990) (Fig. 1A). The Smart Tracker Software (BTS) was used to reconstruct raw kinematics and force data. Joint angles (inverse kinematics) and torques (inverse dynamics) were determined using Smart Analyzer and Smart Clinics Software (BTS). Kinematic and force plate data were filtered using a Low-Pass Butterworth zero-lag 4th-order filter with 12 Hz and 30 Hz cutoff, respectively.

Each subject walked independently at their self-selected speed along a ten-meter walkway for five successful trials without support (i.e., without crutches or walkers). Only tests performed without incidental mistakes, with the subject performing the task naturally with one foot on each force platform during the double support, were analyzed. A picture of the walking gait is shown in Fig. 1B, extracted from the movie available at https://figshare.com/articles/media/hansen_gait_mp4/22335631.

2.3. Data processing

In each trial, ground reaction forces (GRF), kinematics, and torques were normalized for 0 to 100% of the gait cycle. An average of five trials was used to represent each subject. GRF, vertical moments, and ankle work were normalized by the subject's body weight. Gait parameters (Table 1) were compared between the affected (AL) and the unaffected legs (UNL) of HG and between the right leg from the CG and both legs of HG. Previous studies on drop foot gait also analyzed only the right leg of controls (Bidabadi et al., 2019; Błażkiewicz and Wit, 2019). A symmetry index (SI) was calculated for AL and UNL for HG, and right (RL) and left limbs (LL) for CG, according to Queen et al. (2020). A negative value indicates, for each parameter, that AL < UNL and LL < RL. BTS Smart Clinics software reports pelvis data for the right and left gait cycles, averaged for the analysis reported here.

For principal component analysis (PCA), 31 discrete gait parameters shown in Table 1 were normalized to zero average and unitary standard deviation and stored in the columns of a matrix **E** [39 × 31]. According to Schutte et al. (2000), choosing discrete gait variables is inherently arbitrary in calculating the normality index. A group of experienced clinicians was consulted to determine an appropriate set of variables.

Each row of **E** corresponded to the 31 gait parameters associated with AL from HG (12 subjects), the UNL from the same group (12 subjects), and the right leg from CG (15 subjects), totalizing 39 rows. PCA

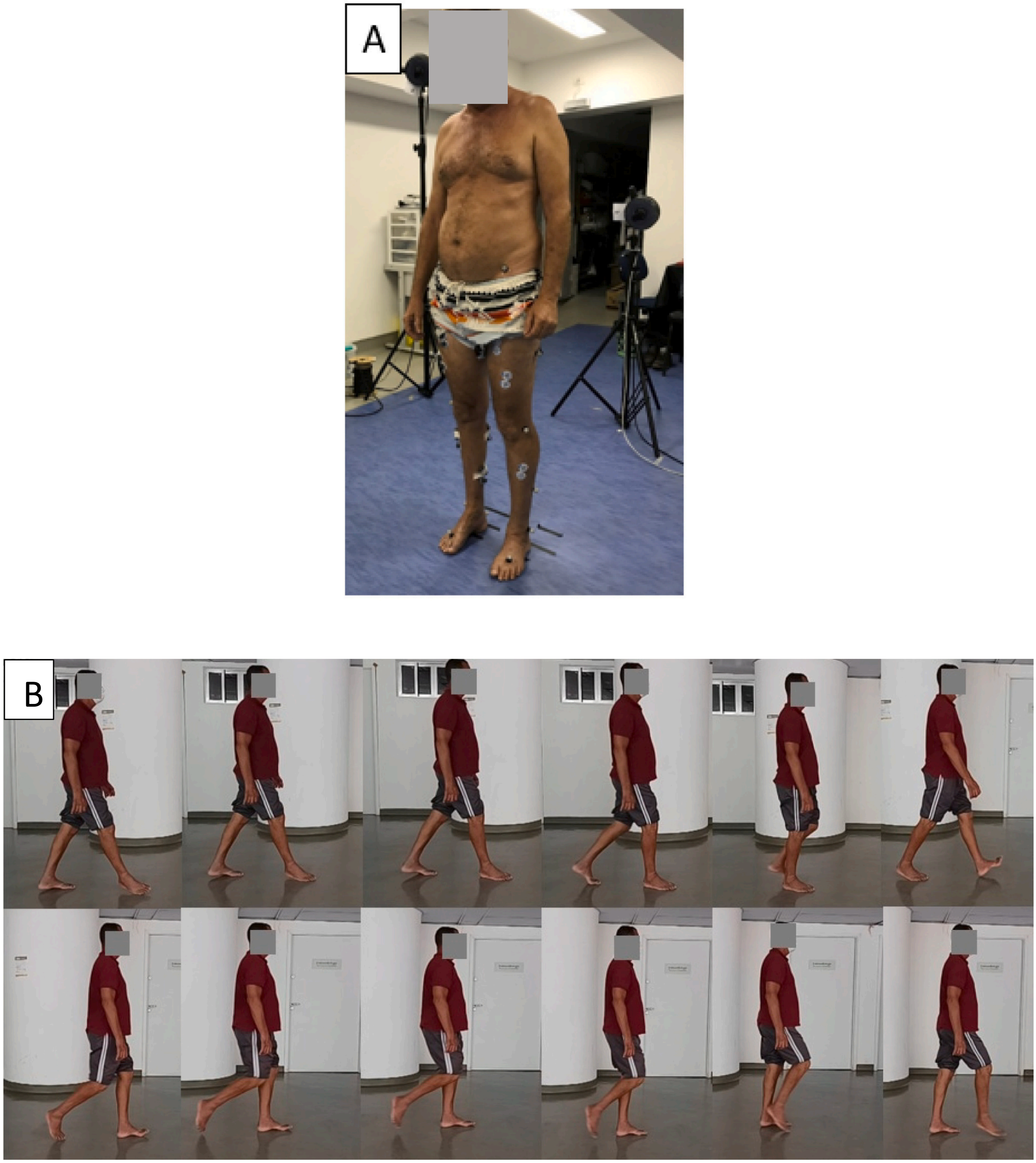

Fig. 1. Anatomical marker set protocol (A) and walking gait picture (B) – movie available at https://figshare.com/articles/media/hansen_gait_mp4/22335631

decomposes the covariance matrix **S** [31 × 31] of **E** into a **PC** [31 × 31] matrix of principal components (PCs), where each column contains the loading factors of **PC** eigenvectors that represent the linear combinations of the 31 gait parameters. The columns of **PC** are arranged in descending order of component variance (Jolliffe, 2002). Each component's relative importance, or variance, is expressed in a vector of 31 eigenvalues corresponding to PCs. Usually, the first PCs retaining 80% of total data variation are selected for further analysis (McKean et al., 2007).

To determine the relative variance contribution of each principal component (PC), the corresponding eigenvalue is divided by the sum of all eigenvalues. In our study, we retained the first six PCs. Additionally, PCA generates a matrix of PC scores denoted as **SC** [39 × 31], which represents the data stored in **E** on the principal component space. The rows of **SC** correspond to observations, while columns represent components. To obtain **SC**, the **PC** columns are demeaned and multiplied by the square root of the corresponding eigenvalues (Jolliffe, 2002). Differences between AL and CG were evaluated by comparing their PC scores (Chester and Wrigley, 2008). The loading factors of corresponding PC scores with statistical differences between HG and CG were visually analyzed to aid in interpreting the information attained by PCs. Loading factors >80% were deemed relevant (Muniz and Bini, 2017).

Table 1
The 31 input measures considered in PCA analysis.

Variable number	Variable	Unit	Variable number	Variable	Unit
Ankle			**GRF**		
1	Ankle angle at initial contact	deg	18	First vertical peak	% BW
2	Maximal dorsiflexion in stance	deg	19	Second vertical Peak	% BW
3	Maximal plantar flexion in stance	deg	20	Braking anteroposterior peak	% BW
4	Maximal dorsiflexion in swing	deg	21	Propulsive anteroposterior peak	% BW
5	Maximal pronation in stance	deg	22	Maximal medial force	% BW
6	Maximal supination in stance	deg	23	Maximal Lateral force	% BW
Knee			**Moment**		
7	Maximal flexion in stance	deg	24	Maximal plantar flexor torque	*Nm/ Kg*
8	Maximal flexion in swing	deg	25	Maximal knee extensor torque	*Nm/ Kg*
9	Frontal plane amplitude in stance	deg	26	Maximal hip flexor torque	*Nm/ Kg*
Hip			27	Maximal hip extensor torque	*Nm/ Kg*
10	Maximal hip flexion in stance	deg	**Total work**		
11	Maximal hip extension in stance	deg	28	Net ankle work in stance	J/kg
12	Maximal hip flexion in swing	deg	**Temporal variables**		
13	Maximal adduction in stance	deg	29	Percentage stance time	%
14	Maximal abduction in stance	deg	30	Percentage swing time	%
Pelvis			31	Gait speed	m/s
15	Pelvic tilt range	deg			
16	Pelvic obliquity range	deg			
17	Pelvic rotation range	deg			

To define a hyperelliptic boundary in the PC-hyperspace for the control group, we normalized their scores by the respective variance (Flury and Riedwyl, 1986; Muniz et al., 2012). We used the standard distance to estimate how much our patients deviated from normality, which can be interpreted as the mean difference in standard deviation units. Consequently, we created a normality index defined as the standard distance between the scores of each patient's limb (AL or UNL leg) to the hyperelliptic boundary center in the control group's PC-hyperspace.

2.4. Statistical analysis

The Shapiro-Wilk test was used to test for data normality. The independent *t*-test or the Mann-Whitney test was used to compare the average gait parameters and PC scores between groups of subjects (HG and CG) for parametric or nonparametric data, respectively. The paired t-test or Wilcoxon signed-rank test was also performed to compare the AL and UNL of HG (Simonsen et al., 2010). The significance level was set at $\alpha < 0.05$. The magnitude of differences was calculated using Cohen's effect size (d) for normally distributed data and r effect size otherwise. The interpretation of d was 0.20 (small), 0.50 (medium), and 0.80 (large) and, for r, 0.10 (small), 0.30 (medium), and 0.50 (large) (Cohen, 1992). The statistical analysis was performed using SPSS 28.0.0.0 (SPSS, USA).

3. Results

3.1. Parametric analysis

Parametric analysis showed that the HG had an increased maximum plantar flexion angle at initial and terminal contacts and during the swing in AL compared to UNL and controls (Table 2 and Fig. S-1 of the Supplementary Material). Additionally, both legs of the HG had a higher knee frontal plane amplitude, while the UNL showed a smaller hip adduction peak angle during stance compared to the CG. The HG also had a higher pelvic tilt range than the CG.

The HG walked slower than the controls (Table 3), with a lower stance phase percentage on the AL compared to the UNL and the CG. Correspondingly, an increased percentage of swing duration was observed in the AL compared to the UNL. The AL presented a lower vertical second force peak than the UNL and the controls (Table 3 and Fig. S-2). Moreover, the UNL showed a higher supination force (lateral peak) than the CG. The inverse dynamics analysis (Table 3 and Fig. S-3) revealed in the AL, compared to controls, there was a reduced ankle plantar flexor torque in the terminal stance, and net ankle work during stance (Table 3).

Most parameters showed higher SI (<10%) in the HG (Tables 2 and 3), with larger values in ankle angle at initial contact and maximal dorsiflexion in swing (Table 2). At the same time, the control group showed an acceptable SI in most variables.

3.2. Multivariate analysis

The PCA retained the first six PCs (Fig. 2A, C and E) to calculate the standard distance, accounting for 80.7% of data variance. Statistical analysis revealed that the standard distance differed significantly between the CG, UNL, and AL groups, with the CG group having shorter distances than the UNL and AL groups (Table 3). Notably, the AL group had a larger standard distance than the UNL group (Fig. 2A, C and E), suggesting that gait patterns were modified in both groups, but to a greater extent in the AL group.

Further analysis indicated that only the first ($p = 0.018$), the third ($p = 0.016$), and the fourth ($p = 0.006$) PC scores presented significant differences between the controls and the HG AL. The first eigenvector (Fig. 2B) identified key differences between the two groups, including ankle angle at initial contact (Variable 1 of Table 1), maximal plantar flexion in stance (Var. 3), maximal dorsiflexion in swing (Var. 4), and percentage swing time (Var. 31). The third eigenvector highlighted differences in the first peak of force (Var. 19) and net ankle work in stance (Var. 28) (Fig. 2D), while the fourth detected differences in percentage stance time (Var. 29) (Fig. 2F). No significant differences were observed between groups for the remaining eigenvectors.

4. Discussion

The aim of this study was to investigate the gait pattern of patients with leprosy and foot drop as a secondary disability, focusing on kinematics, dynamics, and ground reaction force (GRF). The patients' affected limb gait patterns were compared with the unaffected limb and control participants. A PCA decomposition was used to analyze the scores of gait variables, along with global normality and symmetry indices.

The results showed that patients with foot drop exhibited changes in their gait patterns of both legs compared to control participants (Fig. 2), consistent with previous studies on foot drop caused by other pathologies. Specifically, the patients had a reduced gait speed and stance time percentage, and an increased swing time percentage. Patients also

Table 2
Kinematic gait parameters (mean ± standard deviation).

	HG			CG		*P/ES* (ALxUNL)	*P/ES* (ALx CG)	*P/ES* (UNLx CG)
	AL	UNL	SI	RL	SI			
ANKLE								
Ankle angle at initial contact (*deg*)	−16.8 ± 8.3	−6.6 ±10.3	−70.0%	−5.4 ± 2.5	5.1%	**0.01***/ d = 1.09	**0.02***/ **d = 1.85**	0.704/ d = 0.16
Maximal dorsiflexion in stance (*deg*)	11.6 ± 3.7	11.8 ± 4.9	6.9%	10.2 ± 2.5	3.0%	0.433/ *r* = 0.16	0.384/ *r* = 0.07	0.264/ d = 0.41
Maximal plantar flexion in stance (*deg*)	−29.1 ± 11.5	−14.6 ±11.6	−38.2%	−18.8 ± 5.8	−2.2%	**0.018***/ **d = 1.25**	**0.023***/ **d = 1.13**	0.286/ d = 0.45
Maximal dorsiflexion in swing (*deg*)	−12.4 ± 6.2	2.4 ± 7.6	−137.5%	−1.4 ± 3.9	−8.8%	**0.041***/ ***r* = 0.41**	**<0.001***/ ***r* = 0.79**	0.115/ d = 0.62
Maximal pronation in stance (*deg*)	−6.4 ± 5.2	−5.9 ± 2.8	12.9%	−5.0 ± 2.1	−9.2%	0.534/ *r* = 0.12	0.892/ *r* = 0.02	0.397/ *r* = 0.17
Maximal supination in stance (*deg*)	7.8 ± 4.3	7.7 ± 4.4	0.12%	5.2 ± 2.0	−7.1%	0.704/ d = 0.02	0.081/ d = 0.77	0.123/ d = 0.73
KNEE								
Maximal flexion in stance (*deg*)	15.5 ±10.0	17.4 ± 8.6	0.5%	13.3 ± 4.6	−3.1%	0.534/ d = 0.20	0.497/ d = 0.28	0.125/ d = 0.59
Maximal flexion in swing (*deg*)	55.9 ± 17.4	51.8 ±12.8	1.3%	57.2 ±11.2	4.8%	0.754/ *r* = 0.06	0.959/ *r* = 0.01	0.799/ *r* = 0.05
Frontal plane amplitude in stance (*deg*)	12.6 ± 9.3	10.6 ± 5.5	4.8%	6.1 ± 2.9	−2.8%	0.476/ d = 0.26	**0.046***/ **d = 0.94**	**0.047***/ **d = 1.02**
HIP								
Maximal hip flexion in stance (deg)	32.1 ± 10.8	34.2 ±10.8	−5.5%	32.3 ± 7.3	−2.5%	0.279/ d = 0.19	0.939/ d = 0.02	0.605/ d = 206
Maximal hip extension in stance (*deg*)	−5.9 ±11.3	−6.7 ±10.0	24.9%	−6.0 ± 6.4	6.0%	0.649/ d = 0.07	0.964/ d = 0.01	0.835/ d = 0.08
Maximal hip flexion in swing (*deg*)	39.4 ± 11.8	36.4 ±11.0	7.3%	34.8 ± 6.7	−0.9%	0.433/ r = 0.16	0.180/ *r* = 0.27	0.237/ *r* = 0.23
Maximal adduction in stance (*deg*)	3.4 ± 4.9	3.1 ± 5.1	54.1%	6.4 ± 2.9	9.8%	0.843/ d = 0.05	0.09/ d = 0.75	**0.043***/ **d = 0.72**
Maximal abduction in stance (*deg*)	−7.9 ± 4.8	−6.6 ± 2.6	−7.4%	−6.1 ± 3.4	3.5%	0.425/ d = 0.33	0.308/ d = 0.43	0.689/ d = 1.6
PELVIS								
Tilt range (*deg*)	6.8 ± 5.1			5.7 ± 3.1		**0.002/*r* = 0.50**		
Obliquity range (*deg*)	6.9 ± 2.8			8.1 ± 5.0		0.807/r = 0.23		
Rotation range (*deg*)	11.1 ± 4.4			11.4 ± 3.9		0.882/d = 0.07		

HS - Leprosy group; AL – Affected limb; UNL – Unaffected limb. CG – control group; RL - right leg. SI – symmetry index; negative value indicates that AL < UNL and left limb < RL. * Values in bold indicate significant differences. *P*-value (p), Cohen's effect size (ES) (d) and effect size r for nonparametric data (r). Positive angles (+) flexion; dorsiflexion; adduction and foot supination. Negative angle (−) extension; plantarflexion; abduction, and foot pronation.

showed a decrease in sagittal ankle range of motion, plantar flexor torque, and net ankle work, especially in the AL, as previously observed in foot drop caused by other pathologies (Kinsella and Moran, 2008; Newman et al., 2007; Voigt and Sinkjaer, 2000; Wiszomirska et al., 2017). These results support our initial hypotheses. Additionally, the patients showed an increased knee frontal plane angular amplitude, reduced hip adduction, and an increased pelvic tilt range. Most of these modifications were observed in both parametric (Tables 2 and 3) and multivariate analyses (Fig. 2).

4.1. Symmetry

The study also examined the symmetry of gait patterns in patients with foot drop. The results showed increasing PCA-based standard distances from the UNL to the AL (Table 3), along with a higher symmetry index (SI) in the HG, indicating an asymmetric gait pattern with a worsening in the AL, as reported in previous studies (Balaban and Tok, 2014; Chen et al., 2005). The largest SIs were observed in ankle motion, hip extension and adduction, horizontal GRFs, plantar flexion torque, knee and hip extensor torques, and net ankle work (Tables 2 and 3). Conversely, the control group exhibited markedly lower SI values. Symmetry is an important indicator of gait health, and the lack of symmetry can affect proper walking technique (Kutilek et al., 2014). Rehabilitation professionals aim to restore a symmetrical gait pattern in patients with foot drop (Nadeau, 2014)

4.2. Gait speed and temporal variables

The results indicated that the HG patients walked 21% slower than controls (Table 3), which is consistent with previous studies on other clinical conditions (Balaban and Tok, 2014; Li et al., 2018; Wiszomirska et al., 2017). Gait speed is a clinical measurement that reflects overall gait performance (Balaban and Tok, 2014; Middleton et al., 2015). A slower gait pattern may be an adaptation to reduce the risk of falls (Van Iersel et al., 2007) by adopting a more cautious gait pattern with hobbling (Wiszomirska et al., 2017). Decreased velocity is likely the result of multiple factors, including debilitated neural control, impaired swing, and reduced muscle strength and mobility (Chen et al., 2005). It negatively affects independence and lowers the quality of life (Ekström et al., 2011). Previous studies have shown that knee torque is closely related to gait speed in normal subjects (Kirtley et al., 1985; Oberg and Karsznia, 1994), but in this study, only plantar flexion torque showed differences between groups.

Furthermore, the AL had a decreased percentage of stance time and an increased swing time (Table 3), similar to previous studies on Duchenne muscular dystrophy (Goudriaan et al., 2018) and stroke (Nadeau, 2014). Additionally, an analysis of the ground reaction force showed that the AL patients had a reduced second peak of force and ankle plantar flexor torque (Table 3), as well as an increased first peak of force (Fig. 2D). These findings suggest difficulty controlling swing during stance on the AL (Kim and Eng, 2003). Consequently, the UNL might need to be quickly oscillated to bear weight on the good safe side (Lauzière et al., 2014), which might explain the instability during weight transfer on the limb with foot drop.

Table 3
Ground reaction force (GRF), moment, and work parameters. Standard distance from PCA analysis is also included.

	HG			CG		*P/ES* (ALxUNL)	*P/ES* (ALxCG)	*P/ES* (AlxCG)
	AL	UNL	SI	RL	SI			
GRF								
First vertical peak *(%BW)*	101.5 ± 10.9	98.6 ± 5.4	2.0%	97.8 ± 4.0	−2.8%	0.373/ d = 0.33	0.085/ *r* = 0.33	0.222/ *r* = 0.24
Second vertical peak *(%BW)*	98.6 ± 5.2	100.7 ± 8.7	−1.6%	104.1 ± 5.5	0.1%	0.583/ *r* = 0.11	**0.033*/ r = 0.41**	0.467/ *r* = 0.15
Braking peak *(%BW)*	−8.2 ± 3.3	−8.3 ± 2.4	4.3%	−10.0 ± 1.8	−10.4%	0.838/ d = 0.03	0.094/ d = 0.68	0.064/ d = 0.8
Propulsive peak *(%BW)*	10.2 ± 4.4	11.8 ± 3.2	−23.7%	10.7 ± 3.1	−13.6%	0.168/ d = 0.42	0.730/ d = 0.13	0.837/ d = 0.35
Medial peak *(%BW)*	−0.6 ± 1.1	−0.9 ± 1.0	37.9%	−0.6 ± 1.0	−0.9%	0.458/ d = 0.27	0.978/ r = 0.01	0.149/ *r* = 0.29
Lateral peak *(%BW)*	4.1 ± 1.1	4.8 ± 1.0	−18.7%	3.7 ± 1.2	−9.8%	0.169/ d = 0.66	0.362/ d = 0.35	**0.021/ d = 0.99**
MOMENT								
Ankle-Plantar flexor *(Nm/kg)*	0.99 ± 0.3	1.22 ± 0.2	−29.2%	1.24 ± 0.3	−8.5%	0.228/ d = 0.51	**0.037/ d = 0.95**	0.907/ d = 0.09
Knee-Extensor *(Nm/kg)*	0.06 ± 0.31	0.12 ± 0.19	−36.8%	0.06 ± 0.18	−12.5%	0.497/ d = 0.23	0.809/ r = 0.05	0.344/ *r* = 0.19
Hip-Extensor *(Nm/kg)*	0.83 ± 0.53	0.79 ± 0.31	−17.8%	0.70 ± 0.10	−15.3%	0.776/ d = 0.09	0.289/ d = 0.34	0.208/ d = 0.39
Hip-Flexor *(Nm/kg)*	−0.63 ± 0.32	−0.64 ± 0.26	4.0%	−0.88 ± 0.32	−5.1%	0.913/ d = 0.03	0.068/ d = 0.78	0.06/ d = 0.82
TOTAL WORK								
Net ankle work in stance *(J/kg)*	−0.03 ± 5.43	−1.93 ± 7.07	−10.1%	−4.58 ± 5.19	4.7%	0.477/ d = 0.30	**0.04*/ d = 0.85**	0.230/ d = 0.42
TEMPORAL VARIABLES								
Percentage stance	59.7 ± 3.1	64.0 ± 3.2	−6.0%	62.7 ± 2.3	1.2%	**0.021*/ r = 0.49**	**0.016*/ d = 1.099**	0.244/ *r* = 0.241
Percentage swing	39.9 ± 4.1	35.2 ± 4.0	9.6%	37.9 ± 1.8	0.8%	**0.021*/ r = 0.49**	0.168/ d = 0.631	0.063/ *r* = 0.372
Gait speed (m/s)	0.82 ± 0.2			1.05 ± 0.2		**0.003*/ d = 1.15**		
STANDARD DISTANCE	9.76 ± 5.25	5.64 ± 2.4		2.29 ± 0.6		**0.034*/ r = 0.69**	**<0.001*/ r = 1.07**	**<0.001*/ r = 1.00**

HS - Leprosy group; AL – Affected limb; UNL – Unaffected limb. CG – control group; RL - right leg. SI – symmetry index; *a* negative value indicates that AL < UNL and left limb < RL. BW – Body weight. * Values in bold indicate significant differences. p-value (p), Cohen's effect size (d) and effect size r for nonparametric data (r). *Peak moment values are reported.

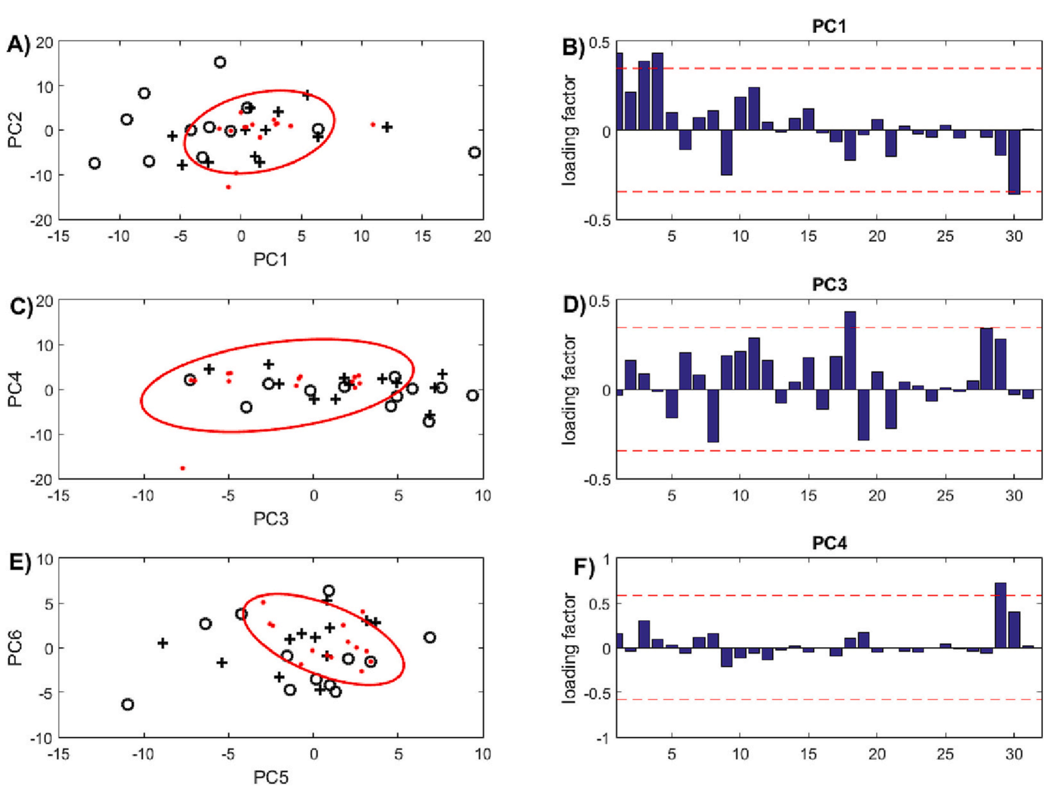

Fig. 2. Scatter plots of principal components scores from CG (red dot), AL (black circle), and UNL (black plus) subjects. First and second (A), third and fourth (C), and fifth and sixth (E) PC scores. The red elliptical boundary corresponds to the CG PCs' 95% confidence interval. The principal component of PCs with statistical differences between CG and AL of HG are PC1 (B), PC2 (D), and PC3 (F). The red horizontal dotted lines corresponded to 80% of loading factors. In the x-axis, the numbers from 1 to 31 correspond to the variables presented in Table 1. (For interpretation of the references to colour in this figure legend, the reader is referred to the web version of this article.)

4.3. Kinematics

The most affected joint in the HG was the ankle in the sagittal plane (Table 2 and Fig. 2B), which is similar to foot drop caused by other diseases (Błażkiewicz and Wit, 2019; Kinsella and Moran, 2008; Newman et al., 2007; Voigt and Sinkjaer, 2000; Wiszomirska et al., 2017). The associated findings include a small ankle dorsiflexion range at heel strike, reduced plantar flexion at the terminal stance, and foot drop in the swing phase. These are primarily caused by weakness of dorsiflexor muscles and spasticity of plantar flexors, whenever present (Dreher et al., 2014; Stewart, 2008). As a result, there is no heel strike at the first contact with the ground in the AL, and the forefoot takes over the load (Wiszomirska et al., 2017). Furthermore, the inability to maintain active dorsiflexion during the swing phase results in foot drop, which affects the energy cost, reduces walking speed, and increases instability and the risk of falls (Miller et al., 2017).

The increase in plantar flexion angle during terminal stance (Table 3 and Fig. 2B) has been observed previously (Balaban and Tok, 2014). Apart from the peroneal nerve, the tibial nerve, which is another branch of the sciatic nerve, is also commonly involved in leprosy due to compression caused by the flexor retinaculum in the tarsal tunnel of the ankle retromalleolar area (Cohen and de Miranda, 2020). This generates an intrinsic foot muscle dysfunction, which plays an essential role during push-off (Balaban and Tok, 2014).

Contrary to previous studies (Wiszomirska et al., 2017), sagittal knee and hip compensations have not been used by the patients to facilitate foot clearance of the affected leg during the swing phase. In a study with Charcot-Marie-Tooth patients with foot drop, Don et al. (2007) found no increased hip and knee flexion during the swing phase. They reported reduced hip and knee flexion during the swing phase. Similarly, Chen et al. (2005) observed reduced knee flexion in the paretic limb during swing in post-stroke hemiparetic patients. In both studies, the primary compensation mechanism for the reduced knee flexion during swing was raising the trunk in pre-swing and swinging with pelvic hiking. In our study, HG increased the pelvic tilt range (Table 2). This finding is associated with balance dysfunction and weight-bearing asymmetry, similar to chronic stroke patients (Karthikbabu et al., 2016).

Inverse dynamics, reaction forces, and energy analyses.

The highest loading factor for the third principal component was observed during the vertical first peak of force (Fig. 2D). Despite having a higher average value for the AL, this variable did not show any statistical differences in the parametric tests (Table 3). Gait discrete parameters cannot account for the high degree of correlation between various aspects of an individual's gait (Tingley et al., 2002), unlike multivariate analysis (Chau, 2001). A large first peak of force is associated with higher gait impact, which can be a risk factor for injuries due to overuse. Altered body geometry during initial contact may reduce shock attenuation (James et al., 2010).

The reduced second peak of ground reaction force in the AL (Table 3), associated with lower ankle plantar flexor torque during terminal stance, is linked with decreased propulsion torque during gait (Newman et al., 2007; Wiszomirska et al., 2017). Previous studies have reported similar results (Bowden et al., 2006; Balasubramanian et al., 2007; Blazkiewicz et al., Wiszomirska et al., 2017). This mechanism provides a slower progression of the body's center of mass over the foot of support, more controlled ankle motion, and increased stability (Voigt and Sinkjaer, 2000; Wiszomirska et al., 2017). The ankle plantar flexor moment is related to the musculoskeletal system's active response, with soleus and gastrocnemius providing vertical support throughout the single-leg stance (Neptune et al., 2001). Loss or impairment of force generation in plantar flexors can impact walking performance (Neptune et al., 2001). Our patients did not show any differences in knee extensor and hip flexor, and extensor torque in the sagittal plane (Table 3), unlike previous studies on other diseases (Wiszomirska et al., 2017). However, HG patients presented an increased knee adduction angle range in both limbs and decreased hip adduction during stance in the UNL. Thus, compensations appear outside the sagittal plane in other joints due to ankle impairment.

Our results show that the AL produced a small negative net ankle work during stance (−0.03 J/kg, plantar flexion work) compared to controls (−4.58 J/kg) (Table 3; Fig. 2D). This suggests a decrease in plantar flexion eccentric contraction during stance.

4.4. Multivariate analysis

The standard distance clearly distinguished between the HG and CG gait patterns and between the patients' AL and UNL (Table 3), with large effect sizes observed in all cases. A reference value for gait normality could be established using the standard distance (2.29 ± 0.6) with consistently increasing distances for the UNL (5.64 ± 2.4) and the AL (9.76 ± 5.25), highlighting the degree to which each subject's AL and UNL deviate from normality (Schutte et al., 2000). As such, the standard distance could be used as an index for tracking disease progression and evaluating treatment effects (Muniz et al., 2012), potentially benefiting individuals with other gait-related conditions.

4.5. Study limitations

Our study is, to our knowledge, the first to report on the gait kinematics and dynamics of foot drop in leprosy using 3D gait analysis, but it has some limitations. The Helen Hayes marker set, as described by Kadaba et al. (1990), only partially reconstructs 3D foot kinematics, particularly for ab/adduction, and does not consider the midfoot and forefoot. Nonetheless, this marker set is still utilized with sufficient accuracy to describe 3D ankle joint complex kinematics and can easily reconstruct the whole lower extremity simultaneously, including the ankle, knee, hip, and pelvis, and has been applied in various foot drop gait studies (e.g., Karunakaran et al., 2019; Simonsen et al., 2010; Wiszomirska et al., 2017).

Another limitation is the sample size. The relatively small number of patients is directly related to the social and economic status of leprosy patients, who have limited mobility and live in vulnerable areas, making it challenging for them to attend and participate in gait analysis studies at the university campus. To better evaluate the efficacy of post-surgical correction of foot drop and gain a more thorough understanding of gait improvement after surgical treatment, comparing our results with those of future studies on post-surgical patients would be valuable.

5. Conclusions

Our patients who were cured of leprosy infection, but still had unilateral foot drop, exhibited slower walking velocity and a reduced stance phase percentage on the AL compared to the UNL and the control group. Additionally, the gait cycle swing percentage and plantar flexion angles in the AL during swing increased compared to UNL. Our patients compensated for the foot drop by walking with a higher pelvic tilt and knee frontal plane range, and reduced hip adduction in the UNL. The AL showed a smaller second vertical reaction force peak, reduced plantar flexor torque, and net ankle work.

PCA analysis calculated a larger standard distance from normality for the AL, followed by the UNL. The PC loading factors indicated that the most significant differences between groups were in ankle kinematics, percentage swing, stance times, the first peak of ground reaction force, and net ankle work during the stance phase. These findings can guide rehabilitation exercises, tendon transfer surgeries, and follow-up treatments for leprosy patients with permanent foot drop.

Declaration of Competing Interest

None.

Acknowledgements

This study was financed by the Coordenação de Aperfeiçoamento de Pessoal de Nível Superior – Brasil (CAPES) – Finance Code 001, by CNPq, FAPERJ, and FINEP.

Appendix A. Supplementary data

Supplementary data to this article can be found online at https://doi.org/10.1016/j.clinbiomech.2023.105983.

References

Balaban, B., Tok, F., 2014. Gait disturbances in patients with stroke. PM R 6, 635–642. https://doi.org/10.1016/j.pmrj.2013.12.017.

Balasubramanian, C.K., Bowden, M.G., Neptune, R.R., Kautz, S.A., 2007. Relationship between step length asymmetry and walking performance in subjects with chronic hemiparesis. Arch. Phys. Med. Rehabil. 88 (1), 43–49. https://doi.org/10.1016/j.apmr.2006.10.004.

Beckmann, N.A., Wolf, S.I., Heitzmann, D., Wallroth, A., Müller, S., Dreher, T., 2015. Cavovarus deformity in Charcot-Marie-tooth disease: is there a hindfoot equinus deformity that needs treatment? J Foot Ankle Res 8, 65. https://doi.org/10.1186/s13047-015-0121-6.

Bidabadi, S., Murray, I., Lee, G.Y.F., Morris, S., Tan, T., 2019. Classification of foot drop gait characteristic due to lumbar radiculopathy using machine learning algorithms. Gait Posture 71, 234–240. https://doi.org/10.1016/j.gaitpost.2019.05.010.

Błażkiewicz, M., Wit, A., 2019. Compensatory strategy for ankle dorsiflexion muscle weakness during gait in patients with drop-foot. Gait Posture 68, 88–94. https://doi.org/10.1016/j.gaitpost.2018.11.011.

Błażkiewicz, M., Wiszomirska, I., Kaczmarczyk, K., Brzuszkiewicz-Kuźmicka, G., Wit, A., 2017. Mechanisms of compensation in the gait of patients with drop foot. Clin. Biomech. 42, 14–19. https://doi.org/10.1016/j.clinbiomech.2016.12.014.

Bowden, M.G., Balasubramanian, C.K., Neptune, R.R., Kautz, S.A., 2006. Anterior-posterior ground reaction forces as a measure of paretic leg contribution in hemiparetic walking. Stroke 37 (3), 872–876. https://doi.org/10.1161/01.STR.0000204063.75779.8d.

Chau, T., 2001. A review of analytical techniques for gait data. Part 1: fuzzy, statistical and fractal methods. Gait Posture 13, 49–66. https://doi.org/10.1016/S0966-6362(00)00094-1.

Chen, G., Patten, C., Kothari, D.H., Zajac, F.E., 2005. Gait differences between individuals with post-stroke hemiparesis and non-disabled controls at matched speeds. Gait Posture 22, 51–56. https://doi.org/10.1016/j.gaitpost.2004.06.009.

Chester, V.L., Wrigley, A.T., 2008. The identification of age-related differences in kinetic gait parameters using principal component analysis. Clin. Biomech. 23, 212–220.

Cohen, J., 1992. A power primer. Psychol. Bull. 112, 155–159. https://doi.org/10.1037//0033-2909.112.1.155.

Cohen, J.C., de Miranda, S.T., 2020. Orthopedic surgical foot Management in Hansen Disease. Orthop Clin North Am 51, 279–291. https://doi.org/10.1016/j.ocl.2019.11.012.

Don, R., Serrao, M., Vinci, P., Ranavolo, A., Cacchio, A., Ioppolo, F., Paoloni, M., Procaccianti, R., Frascarelli, F., De Santis, F., Pierelli, F., Frascarelli, M., Santilli, V., 2007. Foot drop and plantar flexion failure determine different gait strategies in Charcot-Marie-tooth patients. Clin Biomech (Bristol, Avon) 22, 905–916. https://doi.org/10.1016/j.clinbiomech.2007.06.002.

Dreher, T., Wolf, S.I., Heitzmann, D., Fremd, C., Klotz, M.C., Wenz, W., 2014. Tibialis posterior tendon transfer corrects the foot drop component of cavovarus foot deformity in Charcot-Marie-tooth disease. J. Bone Joint Surg. Am. 96, 456–462. https://doi.org/10.2106/JBJS.L.01749.

Ekström, H., Dahlin-Ivanoff, S., Elmståhl, S., 2011. Effects of walking speed and results of timed get-up-and-go tests on quality of life and social participation in elderly individuals with a history of osteoporosis-related fractures. J Aging Health 23, 1379–1399. https://doi.org/10.1177/0898264311418504.

Faul, F., Erdfelder, E., Lang, AG., et al., 2007. G*Power 3: A flexible statistical power analysis program for the social, behavioral, and biomedical sciences. Behav. Res. Methods 39, 175–191. https://doi.org/10.3758/BF03193146.

Ferrarin, M., Lencioni, T., Rabuffetti, M., Moroni, I., Pagliano, E., Pareyson, D., 2013. Changes of gait pattern in children with Charcot-Marie-tooth disease type 1A: a 18 months follow-up study. J Neuroeng Rehabil 10, 65. https://doi.org/10.1186/1743-0003-10-65.

Flury, B.K., Riedwyl, H., 1986. Standard distance in univariate and multivariate analysis. Am. Stat. 40, 249–251. https://doi.org/10.1080/00031305.1986.10475403.

Goudriaan, M., Van den Hauwe, M., Simon-Martinez, C., Huenaerts, C., Molenaers, G., Goemans, N., Desloovere, K., 2018. Gait deviations in Duchenne muscular dystrophy-part 2. Statistical nonparametric mapping to analyze gait deviations in children with Duchenne muscular dystrophy. Gait Posture 63, 159–164. https://doi.org/10.1016/j.gaitpost.2018.04.038.

Hambridge, T., Nanjan Chandran, S.L., Geluk, A., Saunderson, P., Richardus, J.H., 2021. Mycobacterium leprae transmission characteristics during the declining stages of leprosy incidence: a systematic review. PLoS Negl. Trop. Dis. 15 (5), e0009436 https://doi.org/10.1371/journal.pntd.0009436.

James, C.R., Scheuermann, B.W., Smith, M.P., 2010. Effects of two neuromuscular fatigue protocols on landing performance. J. Electromyogr. Kinesiol. 20, 667–675. https://doi.org/10.1016/j.jelekin.2009.10.007.

Jolliffe, I.T., 2002. Graphical representation of data using principal components. Princ. Comp. Analys. 78–110.

Kadaba, M.P., Ramakrishnan, H.K., Wootten, M.E., 1990. Measurement of lower extremity kinematics during level walking. J. Orthop. Res. 8, 383–392. https://doi.org/10.1002/jor.1100080310.

Karthikbabu, S., Chakrapani, M., Ganesan, S., et al., 2016. Relationship between pelvic alignment and weight-bearing asymmetry in community-dwelling chronic stroke survivors. J Neurosci Rural Pract 7, S37–S40.

Karunakaran, K.K., Pilkar, R., Ehrenberg, N., Bentley, K.S., Cheng, J., Nolan, K.J., 2019. Kinematic and functional gait changes after the utilization of a foot drop stimulator in pediatrics. Front. Neurosci. 13, 732. https://doi.org/10.3389/fnins.2019.00732.

Kim, C.M., Eng, J.J., 2003. Symmetry in vertical ground reaction force is accompanied by symmetry in temporal but not distance variables of gait in persons with stroke. Gait Posture 18, 23–28. https://doi.org/10.1016/s0966-6362(02)00122-4.

Kinsella, S., Moran, K., 2008. Gait pattern categorization of stroke participants with equinus deformity of the foot. Gait Posture 27, 144–151. https://doi.org/10.1016/j.gaitpost.2007.03.008.

Kirtley, C., Whittle, M.W., Jefferson, R.J., 1985. Influence of walking speed on gait parameters. J. Biomed. Eng. 7, 282–288.

Krishnamurthy, S., Ibrahim, M., 2019. Tendon transfers in foot drop. Indian J Plast Surg 52, 100–108. https://doi.org/10.1055/s-0039-1688105.

Kutilek, P., Socha, V., Viteckova, S., Svoboda, Z., 2014. Quantification of gait asymmetry in patients with ankle foot orthoses based on hip–hip cyclograms. Biocybernet. Biomed. Eng. 34, 46–52. https://doi.org/10.1016/j.bbe.2013.10.001.

Lauzière, S., Miéville, C., Duclos, C., Aissaoui, R., Nadeau, S., 2014. Perception threshold of locomotor symmetry while walking on a split-belt treadmill in healthy elderly individuals. Percept. Mot. Skills 118 (2), 475–490. https://doi.org/10.2466/25.15.PMS.118k17w6.

Li, S., Francisco, G.E., Zhou, P., 2018. Post-stroke hemiplegic gait: new perspective and insights. Front. Physiol. 9, 1021. https://doi.org/10.3389/fphys.2018.01021.

Marciniak, C., 2013. Fibular (peroneal) neuropathy: electrodiagnostic features and clinical correlates. Phys. Med. Rehabil. Clin. N. Am. 24, 121–137. https://doi.org/10.1016/j.pmr.2012.08.016.

McKean, K.A., Landry, S.C., Hubley-Kozey, C.L., Dunbar, M.J., Stanish, W.D., Deluzio, K.J., 2007. Gender differences exist in osteoarthritic gait. Clin. Biomech. 22, 400–409. https://doi.org/10.1016/j.clinbiomech.2006.11.006.

Middleton, A., Fritz, S.L., Lusardi, M., 2015. Walking speed: the functional vital sign. J. Aging Phys. Act. 23, 314–322. https://doi.org/10.1123/japa.2013-0236.

Miller, L., McFadyen, A., Lord, A.C., Hunter, R., Paul, L., Rafferty, D., Bowers, R., Mattison, P., 2017. Functional electrical stimulation for foot drop in multiple sclerosis: a systematic review and Meta-analysis of the effect on gait speed. Arch. Phys. Med. Rehabil. 98, 1435–1452. https://doi.org/10.1016/j.apmr.2016.12.007.

Ministério da Saúde (BR), 2020. Estratégia nacional para enfrentamento da hanseníase 2019–2022. Accessed: December 5th, 2022. https://www.gov.br/aids/pt-br/centrais-de-conteudo/publicacoes/2020/estrategia-nacional-para-enfrentamento-da-hanseniase-2019-2022/view.

Muniz, A.M.S., Bini, R.R., 2017. Shock attenuation characteristics of three different military boots during gait. Gait Posture 58, 59–65. https://doi.org/10.1016/j.gaitpost.2017.07.037.

Muniz, A.M.S., Nadal, J., Lyons, K.E., Pahwa, R., Liu, W., 2012. Long-term evaluation of gait initiation in six Parkinson's disease patients with bilateral subthalamic stimulation. Gait Posture 35, 452–457. https://doi.org/10.1016/j.gaitpost.2011.11.006.

Nadeau, S., 2014. Understanding spatial and temporal gait asymmetries in individuals post stroke. Int J Phys Med Rehabil 02. https://doi.org/10.4172/2329-9096.1000201.

Neptune, R.R., Kautz, S.A., Zajac, F.E., 2001. Contributions of the individual ankle plantar flexors to support, forward progression and swing initiation during walking. J. Biomech. 34, 1387–1398. https://doi.org/10.1016/S0021-9290(01)00105-1.

Newman, C.J., Walsh, M., O'Sullivan, R., Jenkinson, A., Bennett, D., Lynch, B., O'Brien, T., 2007. The characteristics of gait in Charcot-Marie-tooth disease types I and II. Gait Posture 26, 120–127. https://doi.org/10.1016/j.gaitpost.2006.08.006.

Oberg, T., Karsznia, A., 1994. Joint angle parameters in gait: reference data for normal subjects, 10–79 years of age. J. Rehabil. Res. Dev. 31, 199.

Ooi, W.W., Srinivasan, J., 2004. Leprosy and the peripheral nervous system: basic and clinical aspects. Muscle Nerve 30, 393–409. https://doi.org/10.1002/mus.20113.

Pinzur, M.S., Sherman, R., DiMonte-Levine, P., Trimble, J., 1987. Gait changes in adult-onset hemiplegia. Am. J. Phys. Med. 66, 228–237.

Poage, C., Roth, C., Scott, B., 2016. Peroneal nerve palsy: evaluation and management. J. Am. Acad. Orthop. Surg. 24 (1), 1–10. https://doi.org/10.5435/JAAOS-D-14-00420.

Queen, R., Dickerson, L., Ranganathan, S., Schmitt, D., 2020. A novel method for measuring asymmetry in kinematic and kinetic variables: the normalized symmetry index. J. Biomech. 99, 109531.

Schutte, L.M., Narayanan, U., Stout, J.L., Selber, P., Gage, J.R., Schwartz, M.H., 2000. An index for quantifying deviations from normal gait. Gait Posture 11 (1), 25–31.

Sharma, P., Kar, H.K., Beena, K.R., Kaur, H., Narayan, R., 1996. Disabilities in multibacillary leprosy patients: before, during and after multidrug therapy. Indian J. Lepr. 68, 127–136.

Simonsen, E.B., Moesby, L.M., Hansen, L.D., Comins, J., Alkjaer, T., 2010. Redistribution of joint moments during walking in patients with drop-foot. Clin. Biomech. 25, 949–952. https://doi.org/10.1016/j.clinbiomech.2010.06.013.

Stewart, J.D., 2008. Foot drop: where, why and what to do? Pract. Neurol. 8, 158–169. https://doi.org/10.1136/jnnp.2008.149393.

Tingley, M., Wilson, C., Biden, E., Knight, W.R., 2002. An index to quantify normality of gait in young children. Gait Posture 16, 149–158. https://doi.org/10.1016/S0966-6362(02)00012-7.

Van Iersel, M.B., Ribbers, H., Munneke, M., Borm, G.F., Rikkert, M.G.O., 2007. The effect of cognitive dual tasks on balance during walking in physically fit elderly people. Arch. Phys. Med. Rehabil. 88, 187–191. https://doi.org/10.1016/j.apmr.2006.10.031.

Voigt, M., Sinkjaer, T., 2000. Kinematic and kinetic analysis of the walking pattern in hemiplegic patients with foot-drop using a peroneal nerve stimulator. Clin. Biomech. 15, 340–351. https://doi.org/10.1016/S0268-0033(99)00082-0.

Wilder-Smith, E.P., Van Brakel, W.H., 2008. Nerve damage in leprosy and its management. Nat. Rev. Neurol. 4, 656–663. https://doi.org/10.1038/ncpneuro0941.

Wiszomirska, I., Błażkiewicz, M., Kaczmarczyk, K., Brzuszkiewicz-Kuźmicka, G., Wit, A., 2017. Effect of drop foot on spatiotemporal, kinematic, and kinetic parameters during gait. Appl. Bionics Biomech. 2017, 1–6. https://doi.org/10.1155/2017/3595461.

World Health Organization, 2020. Wkly Epidemiol. Rec. 95, 35.